Adult *Drosophila* sensory neurons specify dendritic territories independently of dendritic contacts through the Wnt5–Drl signaling pathway

Kei-ichiro Yasunaga, Akane Tezuka, Natsuko Ishikawa, Yusuke Dairyo, Kazuya Togashi, Hiroyuki Koizumi, and Kazuo Emoto

Department of Biological Sciences, Graduate School of Science, The University of Tokyo, Bunkyo-ku, Tokyo 113-0033 Japan

Sensory neurons with common functions are often nonrandomly arranged and form dendritic territories in stereotypic spatial patterns throughout the nervous system, yet molecular mechanisms of how neurons specify dendritic territories remain largely unknown. In *Drosophila* larvae, dendrites of class IV sensory (C4da) neurons completely but nonredundantly cover the whole epidermis, and the boundaries of these tiled dendritic fields are specified through repulsive interactions between homotypic dendrites. Here we report that, unlike the larval C4da neurons, adult C4da neurons rely on both dendritic repulsive interactions and external positional cues to delimit the boundaries of their dendritic fields. We identify Wnt5 derived from sternites, the ventral-most part of the adult abdominal epidermis, as the critical determinant for the ventral boundaries. Further genetic data indicate that Wnt5 promotes dendrite termination on the periphery of sternites through the Ryk receptor family kinase Derailed (Drl) and the Rho GTPase guanine nucleotide exchange factor Trio in C4da neurons. Our findings thus uncover the dendritic contact-independent mechanism that is required for dendritic boundary specification and suggest that combinatory actions of the dendritic contact-dependent and -independent mechanisms may ensure appropriate dendritic territories of a given neuron.

Precise patterning of the dendritic fields is essential for the correct wiring of neuronal circuitry. In many cases, after dendrites cover their territory, growth beyond the boundaries of their territory is curtailed in order to prevent any overlap of the receptive fields of neighboring neurons and the consequent compromise of neuronal circuit properties. Indeed, neuronal diseases characterized by the formation of enlarged dendritic fields result in severe mental retardation (Purpura 1975; Kaufmann and Moser 2000). Notwithstanding recent progress in our knowledge of molecular mechanisms that promote dendritic elaboration (Jan and Jan 2010; Puram and Bonni 2013), the cellular and molecular mechanisms that restrain dendrite growth to define appropriate dendritic boundaries are still poorly understood.

In both vertebrates and invertebrates, contact-dependent self-repulsion is likely a common mechanism for dendritic boundary specification (Jan and Jan 2010; Zipursky and Grueber 2013). One good example is the dendritic tiling in retinal ganglion cells (RGCs) of the mammalian retina, in which dendrites of RGCs of the same subtype typically cover the whole retina with minimum overlap, like tiles on a floor (Wassle and Boycott 1991; Masland 2012). Deletion of RGCs causes surrounding neurons to reorient their dendrites toward the depleted area (Perry and Linden 1982), suggesting that mutual repulsion between like dendrites mediates establishment of the RGCs' dendritic boundaries. However, it has also been suggested that certain types of RGCs can define their unique territories independently of the dendrite–dendrite contacts. For example, in Brn3b$^{-/-}$ and Math5$^{-/-}$ retinas in which only ∼10% RGCs are formed, the dendritic arbors of at least two classes of surviving neurons are indistinguishable from normal in shape and size (Lin et al. 2004), raising a possibility that, in addition to the dendritic contact-dependent mechanisms, dendritic contact-independent

Corresponding author: emoto@bs.s.u-tokyo.ac.jp

mechanisms likely function to specify dendritic territories even in a two-dimensional (2D) space.

The *Drosophila* dendrite arborization (da) sensory neurons provide a suitable system for the systematic analysis of dendritic territory development (Parrish et al. 2007; Jan and Jan 2010; Emoto 2012). Similar to mammalian RGCs, dendritic arborizations of larval class IV da (C4da) neurons are confined to the 2D space between the epidermis and muscles, and the dendrites cover the whole epidermis in a complete but nonredundant manner. Several lines of evidence demonstrate that dendritic boundaries in larval C4da neurons are defined by homotypic repulsion between neighboring dendrites. First, C4da dendrites display typical avoidance behaviors when two dendritic branches meet at dendritic boundaries (Grueber et al. 2003; Emoto et al. 2004, 2006). Second, duplication of C4da neurons resulted in a partitioning of the receptive field (Grueber et al. 2003). Last, embryonic ablation of C4da neurons caused the remaining C4da neurons to expand their dendritic fields to occupy the territory of the ablated neurons (Grueber et al. 2003). Genetic studies in C4da neurons have revealed that the contact-dependent dendrite repulsions are mediated by multiple molecules, including cell surface proteins (Gao et al. 2000; Hughes et al. 2007; Matthews et al. 2007; Soba et al. 2007) and intracellular signaling molecules (Emoto et al. 2004, 2006; Koike-Kumagai et al. 2009; Matsubara et al. 2011).

During metamorphosis, the larval dendritic arbors are completely replaced with adult-specific processes as a result of extensive pruning and subsequent regeneration of dendritic trees (Kuo et al. 2005; Shimono et al. 2009; Yasunaga et al. 2010; Kanamori et al. 2015). In this study, we investigated how adult C4da neurons rebuild the dendritic territory and found that, unlike the larval dendrites, adult C4da dendrites specify a dendritic boundary independently of dendritic contacts. Our genetic screen revealed that Wnt5 derived from sternites, the ventral-most region of the adult abdomen, is required for specification of the ventral boundaries of C4da dendrites. We further show that Wnt5 promotes dendrite termination on the periphery of sternites through the Ryk receptor family kinase Derailed (Drl) and the Rho guanine nucleotide exchange factor (GEF) Trio in C4da neurons. Our findings thus reveal a novel role of the Wnt5–Drl signaling pathway in the contact-independent dendritic boundary specification and raise a possibility that multiple distinct mechanisms function in parallel to define the dendritic territories of a given neuron.

Results

Dendritic field organization of adult C4da neurons

During metamorphosis, all three C4da neurons degrade their larval dendrites, and two of them, the dorsal ddaC neuron and the ventro–lateral v'ada neuron, subsequently reconstruct adult-specific dendrites, while the ventral vdaB neuron undergoes apoptosis (Fig. 1A; Kuo et al. 2005; Shimono et al. 2009; Yasunaga et al. 2010). To examine how the remaining two adult C4da neurons recon-
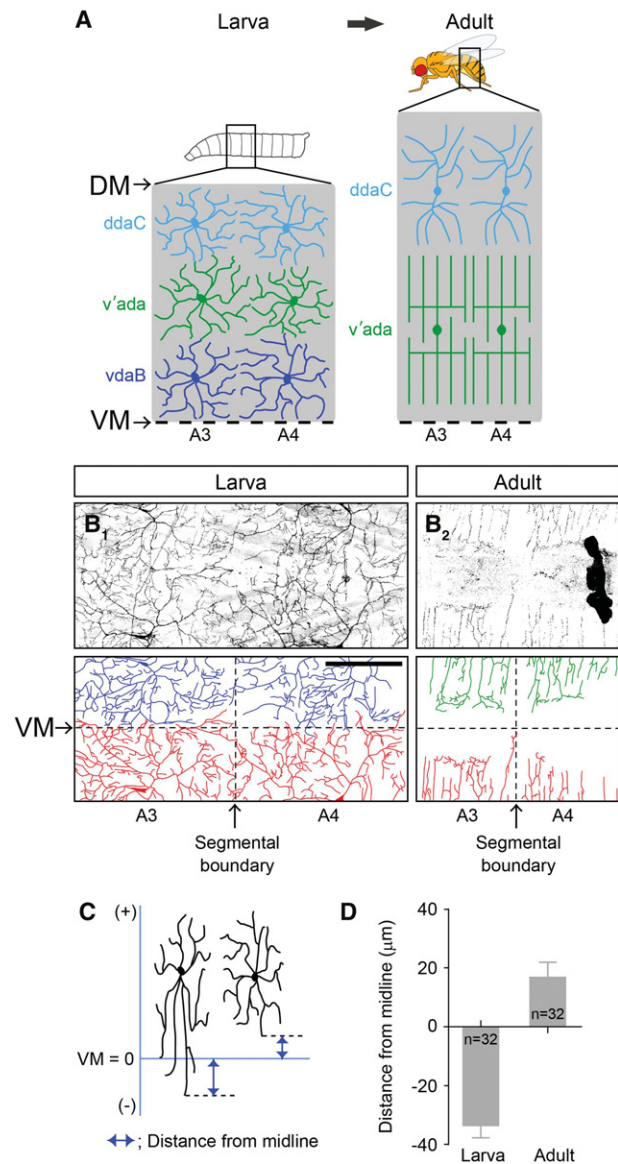
Figure 1. Larval and adult C4da neurons show different coverage of the body wall. (*A*) Schematic depictions of dendritic territories of C4da neurons in two adjacent abdominal segments in the larval and adult stages. The *top* line and the *bottom* dashed line correspond to the dorsal midline (DM) and the ventral midline (VM), respectively. (*B1,B2*) Live images of larval and adult v'ada neurons in the ventral epidermis. (*B1*) Note that dendrites of v'ada neurons show a complete coverage of the body wall. (*B2*) In contrast, in adult flies, v'ada dendrites fail to cover the ventral regions. The horizontal and vertical dashed lines indicate the ventral midline (VM) and the segmental boundary, respectively. Bar, 200 µm. (*C,D*) Quantification of the distance from the ventral midline to the ventral-most dendritic terminals. (*C*) The schema indicates the way to measure the distance. The branches overshooting the ventral midline provide minus values. (*D*) Error bars indicate the standard error of the mean. The numbers *below* each bar indicate *n* values.

struct their dendritic territories on the epidermis, we visualized dendrite organization of C4da neurons by using the C4da neuron-specific *pickpocket* (*ppk*)-Gal4 driving

mCD8GFP (Kuo et al. 2005; Yasunaga et al. 2010; Kanamori et al. 2013). We focused on v'ada neurons that innervate the ventro–lateral epidermis (Shimono et al. 2009; Yasunaga et al. 2010), as the dorsal ddaC dendrites are difficult to image due to tanning of the cuticle. Similar to the larval C4da neurons, adult v'ada neurons positioned their lateral dendritic terminals around the segmental boundaries, and two neighboring dendrites appeared to cover completely the segmental boundaries (Fig. 1B1, B2). To further examine the relative positions of the neighboring dendrites in detail, we stochastically labeled v'ada neurons with EGFP and mCitrine by using the Flybow system (Hadjieconomous et al. 2011). This stochastic labeling experiment clearly showed that adult C4da neurons in neighboring segments cover the segment boundaries with dendrites in a complete but nonredundant manner (Supplemental Fig. S1). In contrast, unlike the larval dendrites, adult v'ada dendrites did not extend to the ventral midline. Instead, growth of adult v'ada dendrites terminated ~20 µm away from the ventral midline (larva, -33.8 µm $\pm$ 3.8 µm, $n = 32$; adult, 17.1 µm $\pm$ 4.8 µm, $n = 32$) (Fig. 1B1–D). As a result, the dendritic fields

of the two adjacent v'ada neurons were separated by ~40 µm, and that space was not covered by C4da dendrites. These data suggest that adult v'ada dendrites might use different mechanisms to specify lateral and ventral boundaries.

Ventral boundaries of adult v'ada dendrites are specified independently of dendrite contacts

To test whether neighboring neurons affect the dendritic boundary specification of adult v'ada neurons, we ablated v'ada neurons in the early pupal stage by using the FLP-out system that induces stochastic expression of the toxic ricin A chain in C4da neurons (Smith et al. 1996). Figure 2B shows an example of a v'ada neuron at the abdominal segment 4 (A4) whose neighboring neurons were ablated. In this situation, both the width and the field size of the v'ada dendrites were significantly expanded compared with those of control v'ada neurons (field size: control, 21.9×10^4 µm^2 $\pm$ 1.1×10^4 µm^2, $n = 6$; ablation, 26.9×10^4 µm^2 $\pm$ 1.1×10^4 µm^2, $n = 9$; width: control, 273 µm $\pm$ 9 µm, $n = 10$; ablation, 352 µm $\pm$ 14 µm, $n = 13$) (Fig. 2A–
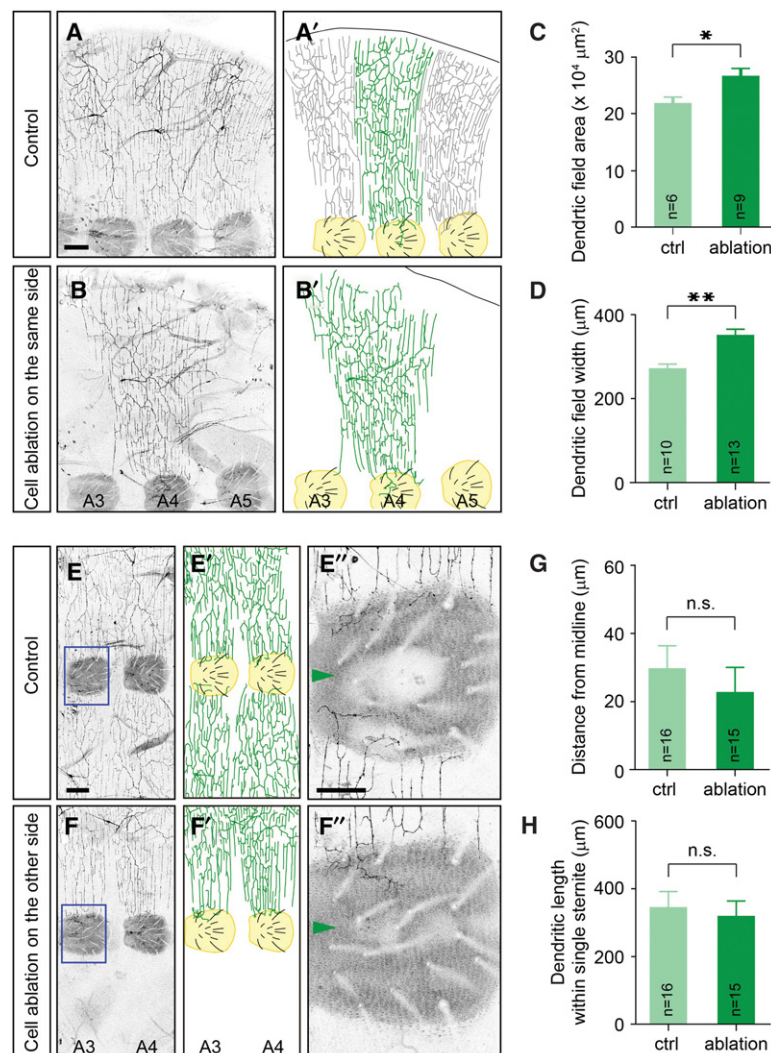
Figure 2. Neighboring neurons are required for proper specification of the lateral boundaries but are dispensable for the ventral boundaries in v'ada neurons. (A,B) Lateral views of adult v'ada dendrites in the A3–A5 segments of an adult ventral abdomen. (A,A') Dendrites of three v'ada neurons cover the body wall completely but redundantly. (B,B') Ablation of neighboring v'ada neurons leads to expansion of dendritic fields of the remaining neuron. Sternites, the ventral-most epithelial region in the adult abdominal segments, are labeled in yellow. Bar, 100 µm. (C, D) Quantification of the dendritic field area (C) and the field width (D) of v'ada neurons in control and cell-ablated abdomens. Error bars indicate standard error of the mean. In C, $P = 0.01$. In D, $P < 0.001$. (E, F) Ventral views of adult v'ada dendrites in A3–A5 segments. (E,E') Ventral boundaries of v'ada neurons are established on the periphery of sternites. (F,F') The ventral boundaries are unaffected by ablation of v'ada neurons in the contralateral hemisegments. Magnified views of the blue boxed regions are shown in E'' and F''. Sternites are labeled in yellow. Bars: E, 100 µm; E'', 50 µm. (G,H) Quantification of the distance from the ventral midline to the branch terminals (G) and the total dendritic length within single sternites (H) in control and cell-ablated abdomens. In G, $P = 0.486$. In F, $P = 0.669$. (*) $P < 0.05$; (**) $P < 0.01$, unpaired Student's t-test.

D). These data suggest that the lateral boundaries of v'ada dendrites are specified at least in part by repulsive interactions between neighboring dendrites. Consistent with these ablation data, time-lapse imaging of dendritic terminals at the segmental boundary revealed the typical avoidance behaviors of dendritic terminals when they met at the segmental boundaries (Supplemental Movie S1). In contrast to the lateral boundaries, ablation of contralateral v'ada neurons had no obvious effect on the relative position of ventral boundaries of v'ada neurons (distance: control, 29.9 µm ± 6.7 µm, $n = 16$; ablation, 22.8 µm ± 7.5 µm, $n = 15$; length: control, 349 µm ± 45 µm, $n = 16$; ablation, 322 µm ± 43 µm, $n = 15$) (Fig. 2E–H), suggesting that the ventral boundaries of v'ada neurons can be specified independently of neighboring dendrites. In both the control and the contralateral ablated cases, the ventral boundaries were coincident on the peripheral of sternites, the ventral-most epithelial region in the adult abdominal segments, which contains arrays of mechanosensory bristles. These data together suggest that dendritic territories of adult v'ada neurons are specified by two distinct mechanisms: Ventral boundaries are specified independently of dendritic contacts, whereas the lateral boundaries are established through repulsive interactions between homotypic dendrites.

Sternites are required to specify the ventral boundaries of adult v'ada dendrites

Adult abdominal segments are subdivided along the dorso–ventral axis into a dorsal tergite, ventro–lateral pleura, and a ventral sternite (Kopp et al. 1999). Given that v'ada neurons positioned the ventral boundaries on the periphery of sternites, we reasoned that sternites might play a role in the establishment of the ventral boundaries. Previous studies reported that the Wingless–Frizzled signaling pathway promotes sternite identity in the adult abdomen and that suppressing the Wingless–Frizzled signaling in the pupal abdomen results in the transformation of sternites into pleura (Shirras and Couso 1996; Kopp et al. 1999). To test the role for sternites in the dendritic boundary specification, we induced somatic clones mutant for both *frizzled* (*fz*) and *frizzled 2* (*fz2*), which are known as the major Wingless receptors in the adult abdomen (Shirras and Couso 1996; Kopp et al. 1999), and successfully generated hemisegments in which sternites were largely transformed into pleura (Fig. 3A,B). In the transformed hemisegments, the dendritic fields of v'ada neurons expanded significantly toward the ventral midline. Importantly, in both the control and transformed cases, the dendritic boundaries of v'ada neurons were consistent with the periphery of sternites (Fig. 3A,B). It is thus likely that sternites are required for correct positioning of the ventral boundaries of v'ada dendrites.

Wnt5 derived from sternites restricts the ventral boundaries of v'ada dendrites

Given that sternites likely play a role in boundary formation, we reasoned that sternites might provide a critical signal for v'ada dendrites to restrict dendritic territories.
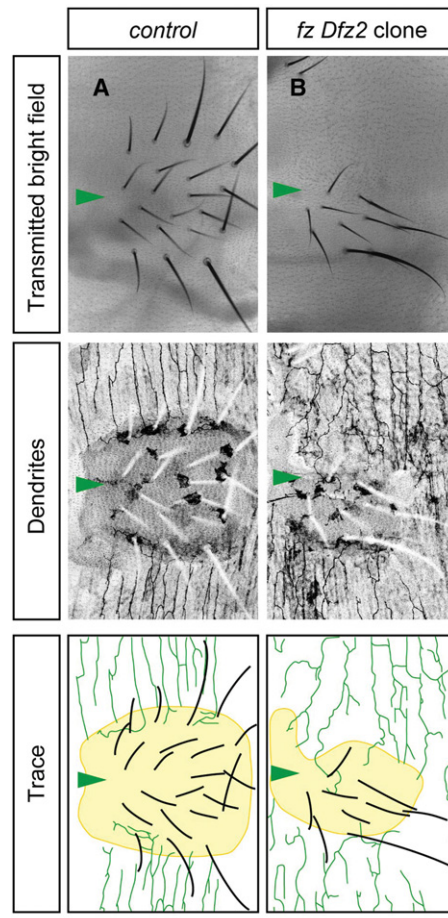
Figure 3. Sternites are required to specify the ventral boundaries of v'ada dendrites. (*A*) Ventral views of sternites in control adult flies. Transmitted bright field (*top*), v'ada dendrites and sternites with bristles (*middle*), and traces (*bottom*) are shown. (*B*) Epithelial clones mutant for both *fz* and *Dfz2* induce partial transformation of sternites into pleura. The dendritic fields of v'ada neurons are extended medially. We examined multiple clones in both wild type ($n = 7$) and *fz Dfz2* ($n = 5$) and found consistent results. Note that in both the control and transformed cases, the ventral boundaries of v'ada dendrites are established on the periphery of sternites. Arrowheads indicate the ventral midline. Bar, 100 µm.

To uncover the potential factors derived from sternites, we carried out a genetic screen, focusing on genes that encode secreted molecules and their receptors (Supplemental Table S1). Among the 37 genes tested, *Wnt5* (also called *Dwnt3*) mutants showed robust defects in ventral boundary formation. Although wild-type dendrites formed their ventral boundaries on the periphery of sternites, dendritic territories of *Wnt5* neurons expanded significantly toward the ventral midline, and dendrites of two v'ada neurons seemed to cover the whole ventral epidermis (distance: wild-type, 20.1 µm ± 4.7 µm, $n = 36$; *Wnt5*, −13.0 µm ± 6.6 µm, $n = 24$; length: wild-type, 778 µm ± 63 µm, $n = 18$; *Wnt5*, 2188 µm ± 107 µm, $n = 12$) (Fig. 4A–D). Interestingly, two v'ada dendrites seemed to tile a sternite with an obvious boundary at the ventral midline (Fig. 4B), suggesting that repulsive interactions
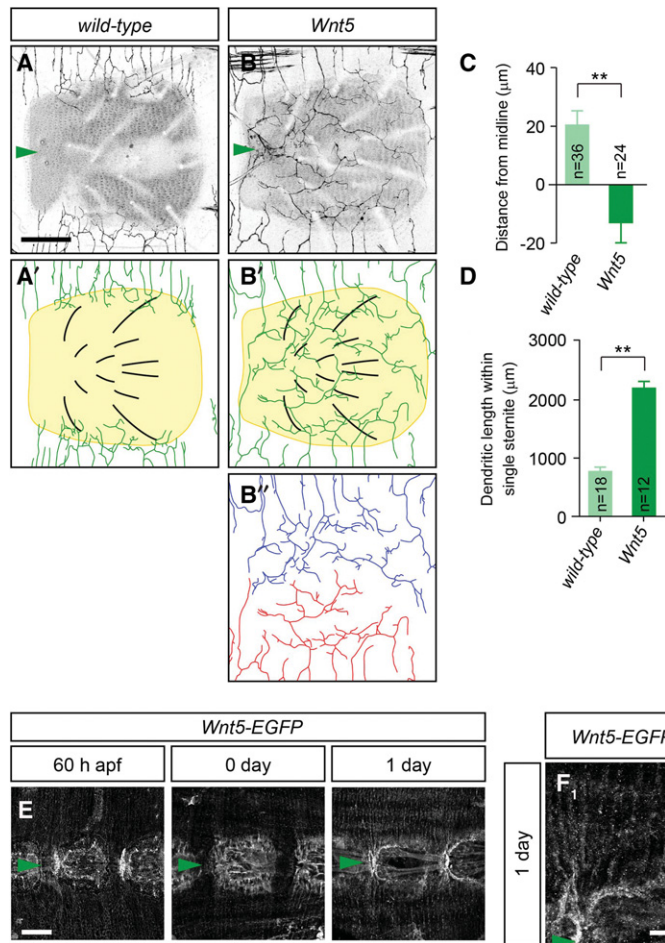
Figure 4. Wnt5 derived from sternites is required for ventral boundary specification of v'ada dendrites. (*A,B*) Ventral views of v'ada dendrites in wild-type (*A,A'*) and *Wnt5* mutant (*B,B'*) adult flies. A trace of *Wnt5* dendrites in a sternite is shown in *B''*. Note that *Wnt5* neurons expand dendritic fields ventrally and cover the whole sternites. Both images were taken in 5-d adult flies. (*C,D*) Quantification of the distance from the ventral midline to dendritic branch terminals (*C*; $P < 0.001$) and the total dendritic length within single sternites (*D*; $P < 0.001$) in wild-type and *Wnt5* mutant flies. (*E*) Wnt5-EGFP expression in abdominal epithelial cells. Representative images in late pupae (60 h after pural formation [APF]; *left*), 0-d adults (*middle*), and 1-d adults (*right*) are shown. Arrowheads indicate the ventral midline. (*F1,F2*) Expression patterns of Wnt5-EGFP (*F1*) and v'ada (*F2*) dendrites in 1-d adults. The outline of the sternites is indicated by the dashed line. Bars: *A,B,F*, 50 μm; *E*, 100 μm. Error bars indicate standard error of the mean. (**) $P < 0.01$, unpaired Student's *t*-test.

between two v'ada dendrites likely specify the boundary. Unlike mutants for the Wingless–Frizzled signaling pathway (Fig. 3), sternites were correctly formed at the ventral-most position in *Wnt5* mutants, suggesting that Wn5 is dispensable for sternite development. Indeed, no significant difference was detectable in the number of bristles and the average size of the sternites (Supplemental Fig. S2G,H). In addition, neighboring *Wnt5* dendrites seemed to cover the whole segmental boundary, which is indistinguishable from that in wild-type dendrites (Supplemental Fig. S2A–D). Further quantitative analysis indicated that the lengths and number of dendritic branches outside of sternites were unaffected in *Wnt5* mutants (Supplemental Fig. S2E,F). Simultaneous observation of C4da dendrites and the extracellular matrix (ECM) suggest that the dendrite–ECM interaction was also unaffected in *Wnt5* mutants (Supplemental Fig. S2I,J). These data suggest that Wnt5 plays a specific role in the establishment of the ventral boundary of v'ada dendrites rather than general roles in dendrite growth and branching.

To investigate temporal and spatial expression patterns of Wnt5 in the pupal/adult abdomen, we generated a novel *Wnt5* reporter line in which EGFP is inserted into the first exon of the *Wnt5* locus (Supplemental Fig. S3). We first examined EGFP expression in the pupal optic lobes, since the anti-Wnt5 antibody detected high levels of Wnt5 in

the medulla of pupal optic lobes (Srahna et al. 2006). Similarly, we found that the Wnt5-EGFP reporter was highly expressed in medulla neurons, and the expression patterns were consistent with the anti-Wnt5 staining, confirming that the Wnt5 reporter mimics expression patterns of endogenous Wnt5 (Supplemental Fig. S3). Using this Wnt5 reporter, we next examined Wnt5 expression in the pupal/adult abdomen. The larval abdomen is reorganized during metamorphosis, and sternites are initially induced ~60 h after pural formation (APF) in the ventral-most region of the pupal abdomen (Kopp et al. 1999). Consistent with sternites functioning as the source for Wnt5, the Wnt5-EGFP reporter signal became visible weakly in the ventral-most abdominal regions ~60 h APF, and the expression levels were gradually increased as the pupa developed to the adult (Fig. 4E). By the 1-d adult stage, EGFP expression was eventually concentrated to the peripheral region of sternites (Fig. 4E). Remarkably, double staining of Wnt5-EGFP and v'ada dendrites revealed that Wnt5 expression is consistent with the ventral boundaries of v'ada dendrites (Fig. 4F1,F2). Taken together, these data suggest that Wnt5 is a sternite-derived factor that specifies the ventral boundaries of adult v'ada dendrites.

To further investigate the role of Wnt5 in dendrite boundary specification, we assessed whether ectopic Wnt5 might affect dendritic boundaries in larval v'ada

neurons. Unlike the adult peripheral tissue, no obvious Wnt5-GFP expression was detectable in larval epithelial cells, whereas larval v'ada neurons express Drl receptor (Supplemental Fig. S4D,E). We ectopically expressed Wnt5 in the larval epithelial cells around which C4da dendrites establish lateral boundaries and found that v'ada dendrites were significantly excluded from the region where ectopic Wnt5 was highly expressed, whereas no obvious growth defect was observed in the region without ectopic Wnt5 (Supplemental Fig. S4A–C). These data suggest that Wnt5 is necessary and sufficient to specify C4da dendrite boundaries.

Wnt5 promotes dendrite termination on the ventral boundary

How might Wnt5 specify the ventral boundary of v'ada dendrites on the appropriate position? One possibility is that dendrites initially innervate into sternites, followed by specific retraction or pruning of the dendritic branches that innervate into sternites, since dendrite pruning/retraction is often observed in developing mammalian sensory circuits to refine dendritic fields (Wong and Ghosh 2002; Emoto 2011). An alternative scenario is that Wnt5 might prevent dendritic branches from innervating sternites. To distinguish between these possibilities, we first measured the

ventral extent of v'ada dendrites during the first 5 d of adult development in wild-type and Wnt5 mutants. At eclosion, no significant difference was observed in both the distance from dendritic terminals to the ventral midline (Fig. 5A) and the dendrite length within single sternites (Fig. 5B) in wild-type controls and Wnt5 mutants. Over the next 24 h, wild-type neurons appeared to reduce dendrite growth, whereas Wnt5 dendrites grew continuously at least during next several days (Fig. 5A,B). Thus, v'ada dendrites appear to avoid sternites, as they initially arrive at the periphery of sternites without going through a noticeable period of invasion followed by retraction/pruning.

To further examine this model, we imaged single v'ada dendrites of live wild-type controls and Wnt5 mutants for 48 h, starting at the time of eclosion. At the 0-d adult stage, many of the terminal branches reached the periphery of sternites in both the wild-type control and Wnt5 mutants (Fig. 5C). Over the next 24 h, Wnt5 dendrites grew into sternites, while wild-type dendrites persisted at the periphery of sternites (Fig. 5C). Quantification of the branch dynamics revealed that dendrite extension was significantly reduced in the wild type over the 48 h, whereas branch extension was much less affected in the Wnt5 mutants compared with wild type (median: 36 μm for 0–1 d and 19 μm for 1–2 d in wild type; 48 μm for 0–1 d and 38 μm for 1–2 d in Wnt5) (Fig. 5D). In contrast,
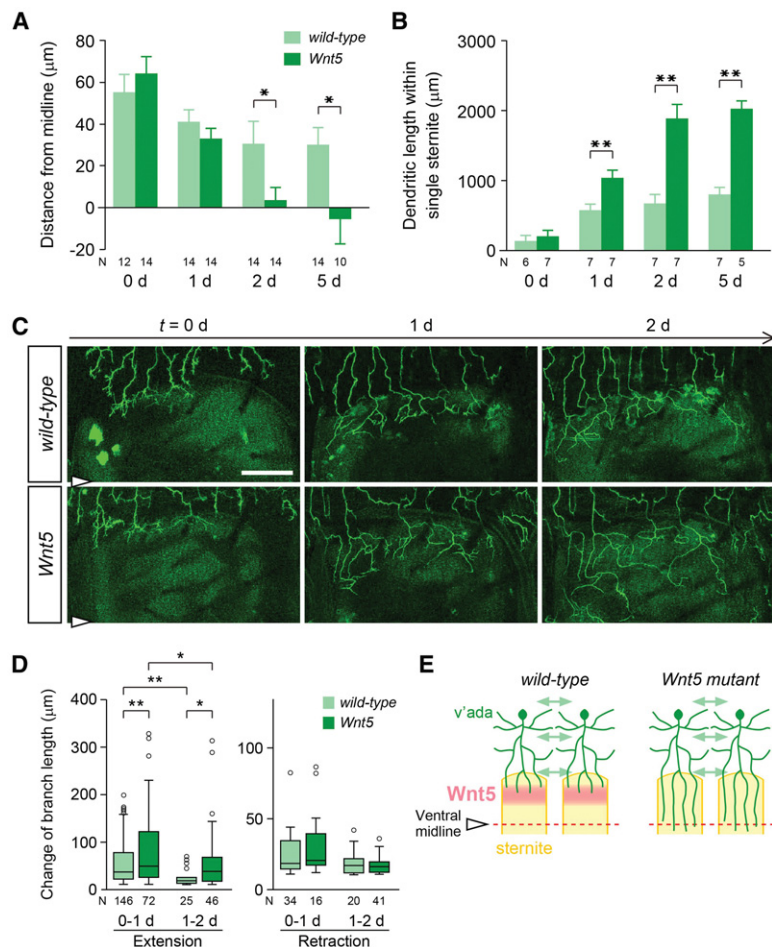
Figure 5. Wnt5 promotes dendrite termination in v'ada neurons. (A,B) Quantification of the distance from the ventral midline to the branch terminals (A) and the total dendritic length within single sternites (B) in wild type (light-green bars) and Wnt5 mutants (dark green bars) in the early adult stages. Error bars indicate standard error of the mean. The numbers below each bar indicate n values. (*) $P < 0.05$; (**) $P < 0.01$, unpaired Student's t-test. (C) Live images of single dendrites from 0- to 2-d adults in wild-type (top) and Wnt5 mutant (bottom) neurons. Bars, 50 μm. (D) Quantification of the changes in branch length in wild-type (light green) and Wnt5 (dark green) dendrites during the 0- to 2-d adult stages. Box plots indicate the median (black line), the 25th and 75th percentiles (box), the data range (whiskers), and outliers (circles). Outliers are defined as data points greater than the 75th percentile of all data points plus 1.5 times the interquartile range. (*) $P < 0.05$; (**) $P < 0.01$, Mann-Whitney U-test. (E) Schematics of dendritic boundary specification for wild type and Wnt5 mutants.

no significant difference was detected in the dendrite retraction between the wild-type controls and *Wnt5* mutants during the 48 h (median: 18 µm for 0–1 d and 17 µm for 1–2 d in wild type; 20 µm for 0–1 d and 15 µm for 1–2 d in *Wnt5*) (Fig. 5D). These observations are consistent with the scenario that *Wnt5* dendrites are able to grow and retract normally but are specifically defective in termination on the periphery of sternites (Fig. 5E).

Drl and Drl-2 receptor kinases in v'ada neurons mediate Wnt5-dependent boundary determination in a redundant manner

Wnt5 typically acts through cell surface receptors on target cells (Fradkin et al. 1995, 2010; Yoshikawa et al. 2003; Kikuchi et al. 2007). To identify the functional Wnt5 re-

ceptors required for dendrite boundary specification in v'ada neurons, we examined nine potential Wnt5 receptors and found that mutants for the Ryk receptor family kinase Drl-2 showed a weak but significant defect in the boundary specification of v'ada dendrites (distance: wild type, 31.9 µm ± 5.2 µm, $n = 28$; *Drl-2*, 8.8 µm ± 5.1 µm, $n = 26$; length: wild type, 808 µm ± 92 µm, $n = 14$; *Drl-2*, 1176 µm ± 93 µm, $n = 13$) (Fig. 6A,C,E,F; Supplemental Table S1). Mutants for Drl, the other member of the *Drosophila* Ryk receptor kinase family, also showed weak boundary defects (distance: *drl*, 29.6 µm ± 6.1 µm, $n = 28$; length: *drl*, 1000 µm ± 106 µm, $n = 14$) (Fig. 6A,B,E,F). We thus next examined *drl Drl-2* double mutants and found robust boundary defects, which were comparable with those in *Wnt5* mutants (distance: *drl Drl-2*, −13.0 µm ± 4.9 µm, $n = 26$; length: *drl Drl-2*, 1847 µm ± 85 µm, $n =$
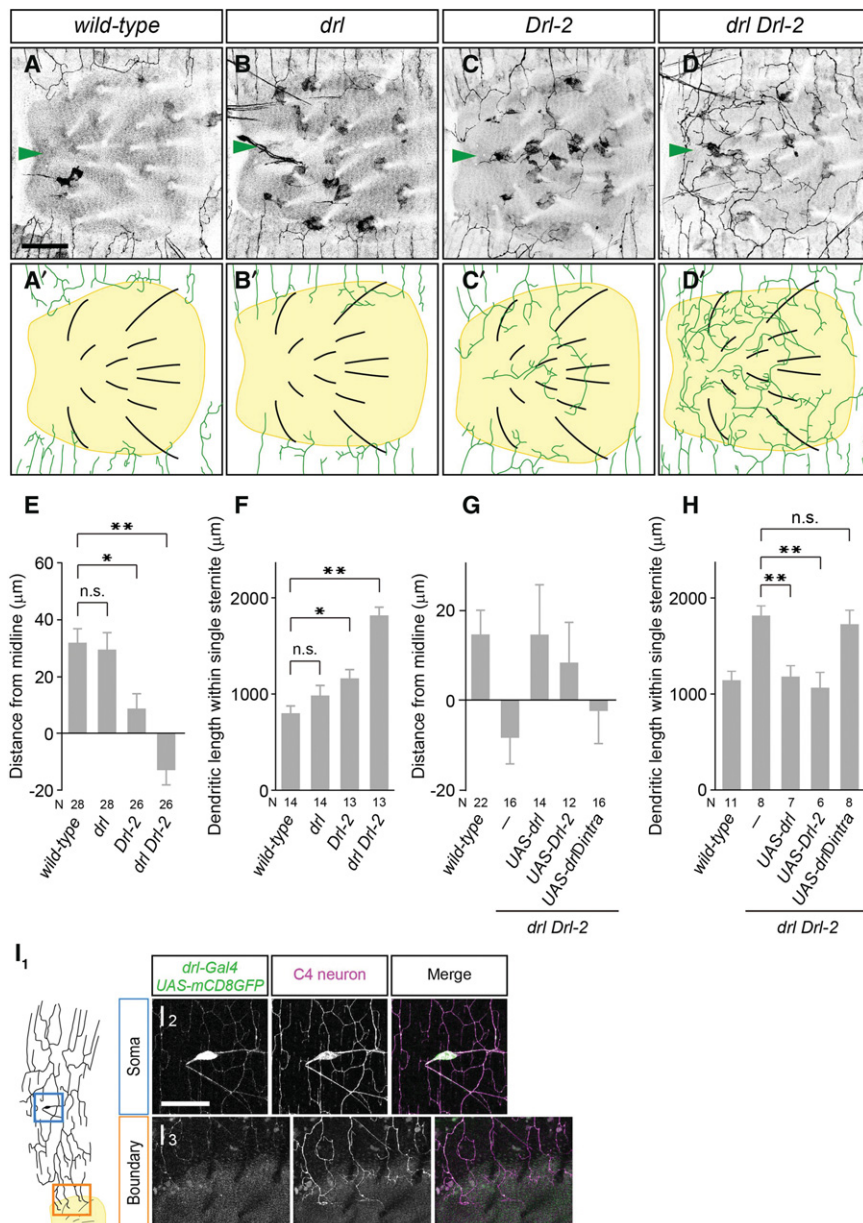
Figure 6. Drl receptor kinases are required for ventral boundary specification in v'ada neurons. (*A–D*) Ventral views of v'ada dendrites in wild-type control (*A*) *drl* mutants (*B*), *Drl-2* mutants (*C*), and *drl Drl-2* double mutants (*D*). Bars, 50 µm. Arrowheads indicate the ventral midline. (*E,F*) Quantification of the distance from ventral midline to dendritic branch terminals (wild-type vs. *drl*, $P = 0.990$; wild-type vs. *Drl-2*, $P = 0.016$; wild-type vs. *drl Drl-2*, $P < 0.001$, one-way ANOVA with Tukey's multiple comparison test) (*E*) and the total dendritic length within single sternites (wild-type vs. *drl*, $P = 0.472$; wild-type vs. *Drl-2*, $P = 0.042$; wild-type vs. *drl Drl-2*, $P < 0.001$, one-way ANOVA with Tukey's multiple comparison test) (*F*). (*G*) Quantification of the distance from the ventral midline to dendritic branch terminals (*drl Drl-2* vs. *drl Drl-2 UAS-drl*, $P = 0.100$; *drl Drl-2* vs. *drl Drl-2 UAS-Drl-2*, $P = 0.333$, one-way ANOVA followed by Dunnett's test). (*H*) Quantification of the total dendritic length within single sternites (*drl Drl-2* vs. *drl Drl-2 UAS-drl*, $P = 0.004$; *drl Drl-2* vs. *drl Drl-2 UAS-Drl-2*, $P = 0.001$, one-way ANOVA followed by Dunnett's test). (*I1–I3*) A schematic of the v'ada dendrites and sternite in the wild-type adult abdomen. (*I1*) Drl expression was visualized with *drl-GAL4 UAS-mCD8GFP* in a 1-d adult. Magnified views of the blue boxed region and the orange boxed region are shown in *I2* and *I3*, respectively. C4da neurons are marked with *ppk* promoter-driven CD4tdTomato. Error bars indicate standard error of the mean. The numbers *below* each bar indicate *n* values. (*) $P < 0.05$; (**) $P < 0.01$.

13) (Fig. 6D–F). Similar to *Wnt5* mutants, *drl Drl-2* double mutants showed no significant defects in the lateral boundary formation (Supplemental Fig. S5A–H). These results suggest that Drl and Drl-2 function together to establish the ventral boundaries of v'ada dendrites.

To examine whether Drl receptors could function cell-autonomously in v'ada neurons to specify the ventral boundary, we performed rescue experiments by expressing *drl* or *Drl-2* in *drl Drl-2* double-mutant neurons. Expression of either *drl* or *Drl-2* driven by *ppk*-Gal4 fully rescued the boundary defects in *drl Drl-2* double-mutant neurons (distance: *drl Drl-2*, −8.6 µm ± 5.4 µm, *n* = 16; +*UAS-drl*, 14.7 µm ± 11.3 µm, *n* = 14; +*UAS-Drl-2*, 8.4 µm ± 9.1 µm, *n* = 12; length: *drl Drl-2*, 1828 µm ± 98 µm, *n* = 8; +*UAS-drl*, 1187 µm ± 111 µm, *n* = 7; +*UAS-Drl-2*, 1064 µm ± 166 µm, *n* = 6) (Fig. 6G,H; Supplemental Fig. S6), indicating that Drl and Drl-2 act cell-autonomously and redundantly in v'ada neurons to specify the ventral dendritic boundaries. Consistent with this notion, RNAi knockdown of *drl* and *Drl-2* in C4da neurons caused boundary defects similar to those in *drl Drl-2* mutants (Supplemental Fig. S5I,J).

Finally, we examined expression patterns of Drl receptors by using the Gal4 enhancer trap in *drl* that has been shown to mimic the expression pattern of *drl* to drive expression of GFP (Moreau-Fauvarque et al. 1998). In adult peripheral tissues, *drl* expression was specifically observed in C4da neurons but not in abdominal muscle fibers and epithelial cells, including sternites (Fig. 6I1–I3), further confirming that Drl receptors function in adult C4da neurons to specify the ventral boundaries. We further examined intracellular distribution of Drl by expressing Drl::GFP in C4da neurons. Drl::GFP seemed to be localized evenly in dendritic arbors as well as axons and the soma (Supplemental Fig. S7).

Rho GEF Trio and Rho1 act with the Wnt5–Drl signaling pathway to specify dendrite boundaries

In many contexts, the Ryk receptor family kinases act through their intracellular domains (Fradkin et al. 2010). Consistently, we found that Drl without the intracellular domain failed to rescue the boundary defects in *drl Drl-2* double-mutant neurons (length: 1727 µm ± 151 µm, *n* = 8) (Fig. 6H), indicating that the intracellular domains of Drl receptors are required for their functions in dendritic boundary specification. Previous studies suggest that Wnt5 signals at least in part through the canonical Wnt signaling pathway (Shimizu et al. 2011). The Src family kinases are also suggested to associate and function with Drl receptors in axon guidance (Wouda et al. 2008). We therefore examined whether attenuation of the canonical Wnt signaling pathway or Src kinase signaling could affect ventral boundary formation and found no significant defects (Supplemental Table S2).

The Rho GTPase GEFs and GAPs (GTPase-activating proteins) function downstream from many receptors to regulate neurite dynamics by controlling the actin cytoskeletons (Luo 2000; Dickson 2001; Bashaw and Klein 2010). In the *Drosophila* genome, 21 potential Rho GAPs and 20 Rho GEFs are present (Bernards 2003). To examine whether Rho GEFs or GAPs might be involved in the dendritic boundary specification, we screened all potential Rho GAPs and GEFs by using RNAi knockdown in neurons and found significant boundary defects in adult v'ada dendrites following knockdown of the Rho GEF *trio* (Supplemental Table S3). To further confirm this, we conducted MARCM (mosaic analysis with a repressive cell marker) analysis to generate *trio* homozygous mutant clones in a heterozygous background (Lee and Luo 1999). We found that *trio* mutant clones showed significant boundary defects in v'ada dendrites (distance: control, 40.0 µm ± 5.1 µm, *n* = 13; *Trio*, −7.3 µm ± 12.1 µm, *n* = 13; length; control, 447 µm ± 37 µm, *n* = 13; *Trio*, 620 µm ± 92 µm, *n* = 13) (Fig. 7A,B,D). These boundary defects in *trio* MARCM clones were fully rescued by expression of the *trio* gene in v'ada neurons (distance: 41.1 ± 8.6 µm, *n* = 13; length: 460 ± 53 µm, *n* = 13) (Fig. 7C–E), indicating that Trio functions autonomously in v'ada neurons.

To investigate whether Trio and Drl receptors might function in the same genetic pathway to regulate ventral boundary formation, we assayed for genetic interactions between *trio* and the Wnt5–Drl signaling genes and found that transheterozygous combinations of mutations in *trio* together with *Wnt5* caused significant boundary defects, whereas heterozygosity for each of the genes had no detectable effect on boundary formation (Supplemental Fig. S9). Similarly, transheterozygous combinations of *trio* and *drl Drl-2* caused significant boundary defects (Supplemental Fig. S9). Thus, Trio and the Wnt5–Drl signaling genes interact genetically to specify dendritic boundaries in v'ada neurons.

Trio could function as a GEF for both Rho1 and Rac1 in a context-dependent manner (Bateman and Van Vactor 2001; Schmidt and Debant 2014). To distinguish between these possibilities, we overexpressed the dominant-negative version of Rho1 or Rac1 specifically in the pupal/adult C4da neurons by using the Flip-out technique (Kanamori et al. 2013). We found that neuronal expression of the dominant-negative Rho1 caused significant boundary defects similar to those seen in *Wnt5* mutants, whereas no obvious boundary defect was apparent following expression of the dominant-negative Rac1 (Supplemental Fig. S10), suggesting that Trio specifies the dendrite boundary through Rho1 activation.

To further examine whether Wnt5–Drl might signal through the Trio–Rho1 pathway to specify the dendritic boundary in v'ada neurons, we next investigated whether overexpression of Trio or a dominant active version of Rho1 in v'ada neurons could rescue the *Wnt5* loss-of-function phenotypes. We found that overexpression of Trio in v'ada neurons significantly rescued the dendritic boundary defects in *Wnt5* mutants (distance: *Wnt5*, −3.8 µm ± 4.2 µm, *n* = 32; *Wnt5 UAS-Trio*, 8.0 µm ± 4.3 µm, *n* = 36; length: *Wnt5*, 1846 µm ± 115 µm, *n* = 16; *Wnt5 UAS-Trio*, 1434 µm ± 125 µm, *n* = 18) (Fig. 7F–K). Similarly, overexpression of the constitutively active Rho1 in *Wnt5* mutant v'ada neurons completely rescued the boundary defects (distance: *Wnt5 UAS-Rho1-CA*, 26.6 µm ± 7.6 µm, *n* = 16; length: *Wnt5 UAS-Rho1-CA*, 1333 µm ± 251 µm, *n* = 8)
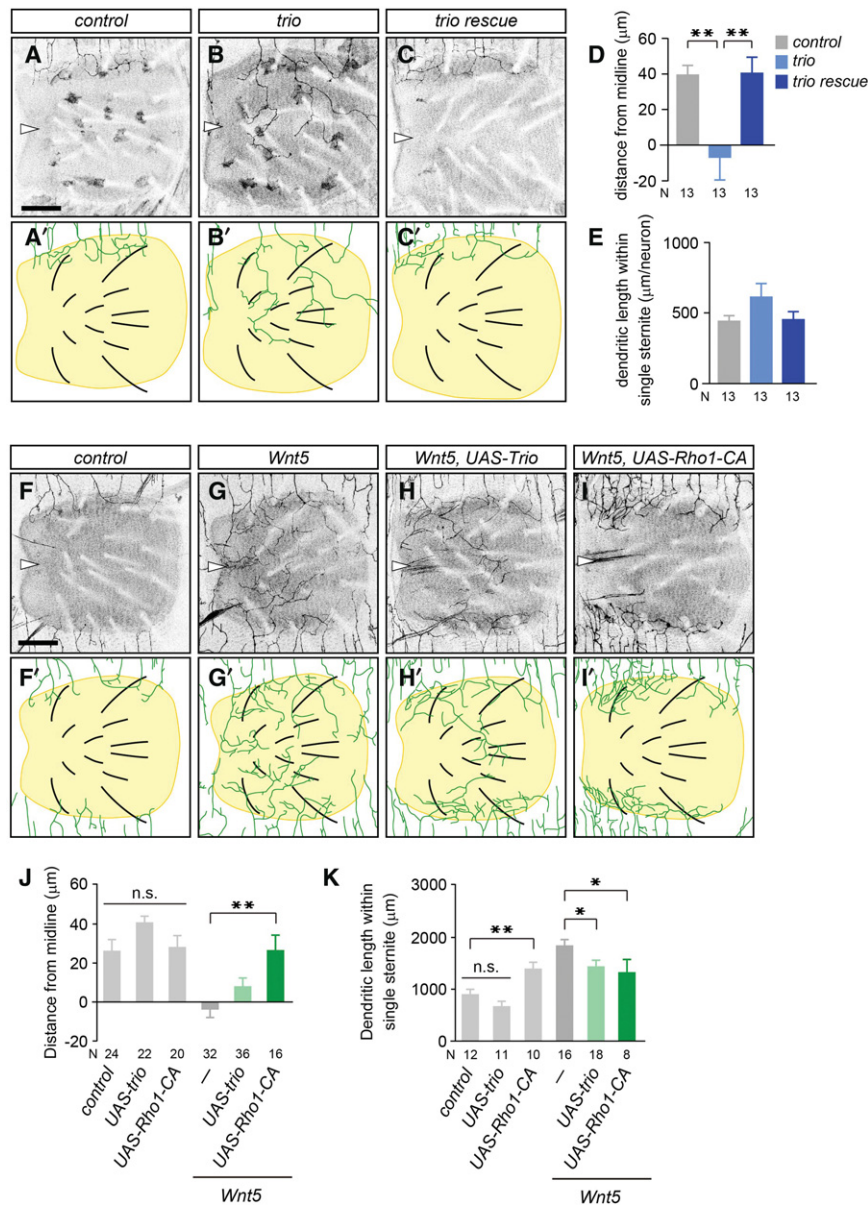
Figure 7. Trio and Rho1 promote dendrite termination downstream from Drl receptors. (*A*–*C*) Ventral views of v'ada dendrites in wild-type control (*A*) and *trio*$^{E4.1}$ (*B*) and *trio*$^{E4.1}$ with a *UAS-trio* transgene (*C*) MARCM clones. Arrowheads indicate the ventral midline. (*D,E*) Quantification of the distance from the ventral midline to the dendritic branch terminals (*D*) and the total dendritic length within single sternites (*E*). Note that we quantified the dendritic length of single neurons. Error bars indicate standard error of the mean. The numbers *below* each bar indicate *n* values. In *D*, control versus *trio*$^{E4.1}$, *P* = 0.002; *trio*$^{E4.1}$ versus *trio* rescue, *P* = 0.002, one-way ANOVA followed by Tukey's HSD test. In *E*, *P* = 0.124, one-way ANOVA. (*F*–*I*) Ventral views of v'ada dendrites in wild-type control (*F*), *Wnt5* mutants (*G*), *Wnt5* mutants with a *UAS-Trio* transgene (*H*), and *Wnt5* mutants with a *UAS-Rho1-CA* transgene (*I*). (*J,K*) Quantification of the distance from the ventral midline to dendritic branch terminals (*J*) and the total dendritic length within single sternites (*K*). The numbers *below* each bar indicate *n* values. In *J*, control versus *UAS-trio* versus *UAS-Rho1-CA*, *P* = 0.115, one-way ANOVA; *Wnt5* versus *Wnt5 UAS-trio*, *P* = 0.081; *Wnt5* versus *Wnt5 UAS-Rho1-CA*, *P* = 0.001, one-way ANOVA followed by Dunnett's test. In *K*, control versus *UAS-trio*, *P* = 0.228; control versus *UAS-Rho1-CA*, *P* = 0.005, one-way ANOVA followed by Dunnett's test; *Wnt5* versus *Wnt5 UAS-trio*, *P* = 0.031; *Wnt5* versus *Wnt5 UAS-Rho1-CA*, *P* = 0.039, one-way ANOVA followed by Dunnett's test. (*) *P* < 0.05; (**) *P* < 0.01.

(Fig. 7I–K). Importantly, overexpression of Trio or the dominant active Rho1 in wild-type v'ada neurons caused no significant defects in the ventral boundary specification of v'ada dendrites (Fig. 7J), suggesting that Trio and Rho1 activities do not simply arrest dendritic growth and/or branching in adult v'ada neurons; rather, Trio and Rho1 specifically promote dendrite termination on the periphery of sternites downstream from the Wnt5–Drl signaling. Taken together, our findings indicate that Wnt5–Drl signaling promotes dendrite termination at least in part through the Trio–Rho1 pathway in adult v'ada neurons.

Discussion

Dendritic territories of sensory neurons in the same functional class are often organized in stereotyped patterns. Previous studies have established that dendritic boundaries of the larval C4da sensory neurons in *Drosophila* are predominantly established through mutual repulsion between neighboring dendrites (Grueber et al. 2003; Emoto et al. 2004). In this study, we showed that, unlike the larval neurons, adult v'ada neurons establish the ventral boundaries independently of neighboring neurons (Figs. 1, 2). Furthermore, our genetic ablation data, in which transformation of sternites to pleura caused the ventral boundaries to extend ventrally (Fig. 3), indicated that sternite-derived factors are required for the ventral boundary specification (Fig. 3). In contrast to the ventral boundary, v'ada neurons required adjacent neurons to define the lateral boundaries, like the larval v'ada neurons (Figs. 1, 2). Thus, v'ada dendrites establish the lateral boundaries through the dendritic contact-dependent mechanism, whereas the ventral boundaries are specified by the contact-independent mechanism.

The cellular mechanisms underlying contact-dependent and -independent boundary determination seem to be distinct. Our time-lapse observations demonstrated that dendritic terminals of adult v'ada neurons remained dynamic to avoid each other at the lateral boundaries even after they established the boundaries (Supplemental Movie S1). This is consistent with the previous report that dendrite boundaries of larval C4da neurons are defined by continuous avoidance behaviors of terminal branches (Emoto et al. 2004). In contrast, in the ventral boundaries, adult v'ada neurons exhibited reduced dendrite dynamics after reaching the boundary on the periphery of sternites and eventually arrested dendrite growth (Fig. 5). Therefore, the contact-independent boundary specification appears to be mediated by dendrite termination, whereas the contact-dependent mechanism is likely mediated by homotypic repulsion. These two mechanisms appear to act independently, since no obvious defects were observed in lateral boundary formation in v'ada dendrites mutant for *Wnt5* and *drl* despite the fact that the ventral boundaries were significantly impaired (Figs. 4, 6).

Recent studies have identified multiple repulsive signaling pathways that function in dendrite patterning of vertebrate and invertebrate neurons, including semaphorin/plexin (Polleux et al. 2000; Matsuoka et al. 2012; Sun et al. 2013), Dscams (Matthews et al. 2007; Soba et al. 2007; Fuerst et al. 2009), protocadherins (Lefebvre et al. 2012), Netrin/DCC/UNC-5 (Smith et al. 2012), and Slit/Robo (Furrer et al. 2007; Gibson et al. 2014). We thus examined potential roles of the repulsive factors in the ventral boundary specification of v'ada dendrites by using genetic mutants or RNAi knockdown, but, to our surprise, none of them showed obvious defects in v'ada dendrite boundary specification (Supplemental Table S1). Instead, using an unbiased genetic screen, we identified Wnt5, a secreted member of the Wnt family proteins, as the critical factor derived from sternites (Fig. 4). We also identified the Ryk receptor family kinases Drl and Drl-2 as the receptors for Wnt5 in v'ada neurons (Fig. 6). These data have demonstrated that Wnt5–Drl signaling plays an essential role in the ventral boundary specification of v'ada dendrites.

How does Wnt5–Drl signaling specify the dendritic boundary at the stereotyped position? In the mouse spinal cord, Wnt5a is expressed by the cells surrounding corticospinal tract axons in a gradient along the anterior–posterior axis, and this Wnt gradient repels corticospinal axons down the spinal cord (Liu et al. 2005). In the present study, we found that Wnt5 expression in the ventral epithelium is dramatically changed during the pupal/adult stage (Fig. 4E). Wnt5 expression was initially visible in epithelial cells around the entire sternite regions at ~60 h APF, but Wnt5 production was gradually restricted to the peripheral region of sternites during the adult stages. In contrast, Drl receptors seemed to be expressed in v'ada neurons throughout the larval-to-adult development at the same level (Fig. 6I). Thus, the spatial and temporal control of Wnt5 expression likely defines the appropriate positioning of the ventral boundary. In addition, our studies using a novel Wnt5 reporter indicated that the ventral dendritic boundaries of v'ada neurons are coincident with the places where Wnt5 is produced (Fig. 4F). Therefore, in spite of its diffusive nature, Wnt5 seems to exert its influence on v'ada dendrites in the vicinity of the protein source. Recent studies indicate that Wnt5a contains multiple lipid modifications, including palmitoylation, and that the lipidation of Wnt5a protein is critical for its functions (Kikuchi et al. 2007). It is thus possible that Wnt5 proteins secreted from sternites might be anchored to cell membranes or nearby in the ECM to produce a sharp boundary for v'ada dendrites at the precise regions. Collectively, it appears likely that the spatiotemporally regulated expression as well as the short-range action enable Wnt5 to define a sharp dendritic boundary at the appropriate timing and positioning.

In the nervous system, Wnt5–Drl/Ryk signaling acts as both attractive and repulsive cues for axons and dendrites presumably through distinct downstream targets, including Src family kinases and CaMKII (Wouda et al. 2008; Hutchins et al. 2011; Wu et al. 2014). Our time-lapse observations revealed that adult v'ada neurons terminate dendrite growth specifically on the periphery of sternites, where Wnt5 is locally produced, without obvious attractive or repulsive responses to the Wnt5 source (Figs. 4, 5). Thus, Wnt5–Drl signaling might limit dendrite growth on the periphery of sternites rather than function as attractive/repulsive cues for v'ada dendrites. Consistent with this scenario, neither Src kinases nor CaMKII was required for the dendrite boundary specification (Supplemental Table S2). Instead, we identified the Rho GTPase GEF Trio and Rho1 as the novel downstream factors that mediate Wnt5–Drl signaling in dendrite termination. This idea is supported by the following lines of evidence. First, reduction of Trio or Rho1 activity in v'ada neurons caused dendrite boundary defects similar to those observed in *Wnt5* mutants (Fig. 7; Supplemental Fig. S10). Second, *Wnt5* and *drl* mutations showed a strong genetic interaction with *trio* mutations in the dendrite boundary specification of adult v'ada neurons (Supplemental Fig. S9). Third, overexpression of Trio or the constitutively active Rho1 in *Wnt5* mutant neurons partially rescued the boundary defects of v'ada dendrites (Fig. 7). This model is consistent with previous reports that loss-of-function mutations in Rho1 and Trio cause *Drosophila* mushroom body neurons to overshoot their dendritic territories, whereas constitutively active Rho1 expression results in a reduction of dendritic fields (Awasaki et al. 2000; Lee et al. 2000). It is also possible that Trio–Rho1 might function in parallel to the Wnt5–Drl signaling in C4da neurons. How Wnt5 activates Trio–Rho1 signaling remains to be elucidated. Given that the intracellular domain of Drl receptor kinases is indispensable for dendrite boundary specification (Fig. 6G,H), Trio could be activated through the intracellular domain of Drl receptors, including the tyrosine kinase domain. Interestingly, recent reports indicate that Trio is phosphorylated at multiple tyrosine residues and that the tyrosine phosphorylations appear to be essential for its Rho GEF activity (DeGeer et al. 2013; Sonoshita et al. 2014). It is thus of interest to test whether Trio could be phosphorylated in response to Wnt5 signals in v'ada neurons.

Developing neurons in the mammalian brain often extend their dendritic arbors into a three-dimensional (3D) space and thus have to establish distinct dendritic boundaries within different environments. Therefore, although mutual repulsion is the most effective way to specify dendritic boundaries when dendrites are confined to the 2D space, multiple systems, including dendritic contact-dependent and -independent mechanisms, are probably required to specify distinct dendritic boundaries in the 3D space. Given that we showed the critical role of Wnt5–Ryk signaling in the contact-independent mechanism for specifying dendritic boundaries in v'ada neurons, it is of great interest to investigate whether the Wnt5–Ryk signaling might play a significant role in establishing the dendritic territories in the 3D space, including the mammalian cortex, as well as in the 2D space, such as retinas. It is worth noting that both Wnt5a and Ryk receptor kinases appear to be expressed in the specific layers of the cortex, the olfactory bulb, and the retinas of the developing mouse brain (Allen Brain Atlas, http://www.brain-map.org).

Materials and methods

Drosophila genetics

Fly stocks and crosses were maintained on standard medium at 25°C unless otherwise stated. The following strains were used: *ppk*-GAL4, *ppk>y+>*GAL4 (Kanamori et al. 2013), *UAS-Wnt5*, *UAS-drl*, *UAS-drlΔICD*, *UAS-Drl-2*, *UAS-trio*, *Wnt5^D7^* (null allele), *drl^R343^* (null allele), *Drl-2^E124^* (null allele), and *trio^E4.1^* (strong hypomorphic allele). *UAS-Rac1-N17*, *UAS-Rho1-N19*, *UAS-Rho1-V14*, *drl*-GAL4^PGAL8^, *ppk-CD4tdTomato*, and *UAS-mCD8GFP* were obtained from the Bloomington *Drosophila* Stock Center and Kyoto *Drosophila* Genetic Resource Center.

To express the ricin proteins in v'ada neurons, we crossed *hsFLP^122^; UFWTRA19/TM6B* flies to *yw; ppk*-Gal4, *UAS-mCD8GFP* flies. The offspring between third instar larval stage and 24 h APF were heat-shocked for 15–30 min at 38°C and dissected at the 15- to 20-d adult stage.

To generate sternite clones, we crossed *ppk-Gal4, UAS-mCD8GFP, hsFLP^122^; FRT 2A/TM6B* flies to *yw; fz^HS1^ fz2^C1^ FRT 2A/TM2* flies.

For the rescue experiments, we crossed *ppk-Gal4 UAS-mCD8GFP; drl^R343^ Drl-2^E124^/CyO* flies to the following stocks: (1) *w; drl^R343^ Drl-2^E124^/CyO; UAS-drl/TM6B*, (2) *w; drl^R343^ Drl-2^E124^/CyO; UAS-Drl-2/TM6B*, and (3) *w; drl^R343^ Drl-2^E124^/CyO; UAS-drlΔICD/TM6B*. These rescue experiments were carried out at 18°C.

For MARCM analysis, v'ada MARCM clones were generated and examined as described previously (Morikawa et al. 2011). Females of *hsFLP^122^, ppk-GAL4 UAS-mCD8GFP; tub-GAL80 FRT2A/TM6B* were mated with males of the following genotypes: (1) *trio^E4.1^ FRT2A/TM6B*, (2) *UAS-trio; trio^E4.1^ FRT2A/TM6B*, and (3) *yw, FRT2A*.

Generation of transgenic flies

We generated the Wnt5-EGFP construct from CH322-141N12 (BACPAC resources) in attB-P[acman]-ApR. CH322-141N12 contains the entire Wnt5 locus plus 5 kb of upstream sequence. We introduced an EGFP-stop/Kmr cassette after the ATG start codon of Wnt5 using the recombineering technique as described (Venken et al. 2006). Potential recombinants were selected on chlor-amphenicol and kanamycin, and the correct targeting of the cassette was verified with PCR. The construct was then introduced into the VK00027 landing site on the third chromosome using φ-C31 integrase (BestGene, Inc.).

Immunohistochemistry

Immunostaining of *Drosophila* abdominal cuticles was performed as described (Yasunaga et al. 2010). Briefly, abdominal cuticles were dissected and fixed in 4% paraformaldehyde in PBS for 30–60 min at room temperature followed by blocking for 60 min in PBS containing 0.3% Triton X-100 and 5% normal goat serum. Tissues were stained with mouse anti-GFP (1:1000; 3F6, Wako), rabbit anti-GFP (1:500; polyclonal, Medical and Biological Laboratories), and/or rat anti-CD8a (1:100; Caltag). Images were taken on a Leica TCS SP8 confocal microscope (Leica) and adjusted for brightness and contrast with Adobe Photoshop (Adobe Systems).

Quantitative analysis

For visualization of dendrites, we labeled v'ada neurons with *UAS*-mCD8GFP under the control of *ppk*-GAL4 and imaged GFP fluorescence in living animals by mounting them in silicon oil (Shin-Etsu) except for Figures 4F and 7G, where immunostaining or the *ppk*-CD4::tdTomato reporter was used. Maximum projections of Z-stacks were used in all cases. The dendrite length was measured by using the ImageJ plug-in NeuronJ (National Institutes of Health). For the quantitative analyses, we focused on the v'ada dendrites in segments A3 and A4, since these neurons exhibit similar and consistent dendrite branch lengths and branch points. For quantification of the total branch length and the branch points, we measured the total branch length of the ventral half of the dendritic fields because the dorsal half partially overlaps with the dendritic fields of the other *ppk*-positive neurons in the same segment. Dendritic fields were defined by a polygon that connected the distal-most dendritic tips (Grueber et al. 2003). For the quantification of the total length of dendritic branches within single sternites, sternites were visualized by taking advantage of their autofluorescence in the green channel. The distance from the ventral midline to the ventral boundaries of C4da dendrites was measured as the distance between the midline and the dendritic terminals located most ventrally.

Statistical analysis

All statistical analysis was performed with Systat 13 (Hulinks, Inc.). For two-sample comparisons, unpaired Student's *t*-tests were applied. For comparisons among more than two groups, one-way ANOVA tests were used and followed by Dunnett's and Tukey's tests, as indicated in the figure legends.

References

Awasaki T, Saito M, Sone M, Suzuki E, Sakai R, Ito K, Hama C. 2000. The *Drosophila* Trio plays an essential role in patterning of axons by regulating their directional extension. *Neuron* **26:** 119–131.

Bashaw GJ, Klein R. 2010. Signaling from axon guidance receptors. *Cold Spring Harb Perspect Biol* **2:** a001941.

Bateman J, Van Vactor D. 2001. The Trio family of guanine-nucleotide-exchange factors: regulators of axon guidance. *J Cell Sci* **114:** 1973–1980.

Bernards A. 2003. GAPs galore! A survey of putative Ras superfamily GTPase activating proteins in man and *Drosophila*. *Biochim Biophys Acta* **1603:** 47–82.

DeGeer J, Boudeau J, Schmidt S, Bedford F, Lamarche-Vane N, Debant A. 2013. Tyrosine phosphorylation of the Rho guanine nucleotide exchange factor Trio regulates netrin-1/DCC-mediated cortical axon growth. *Mol Cell Biol* **33:** 739–751.

Dickson BJ. 2001. Rho GTPases in growth cone guidance. *Curr Opin Neurobiol* **11:** 103–110.

Emoto K. 2011. Dendrite remodeling in development and disease. *Dev Growth Differ* **53:** 277–286.

Emoto K. 2012. Signaling mechanisms that coordinate the development and maintenance of dendritic fields. *Curr Opin Neurobiol* **22:** 805–811.

Emoto K, He Y, Ye B, Grueber WB, Adler PN, Jan LY, Jan YN. 2004. Control of dendritic branching and tiling by the Tricornered-kinase/Furry signaling pathway in *Drosophila* sensory neurons. *Cell* **119:** 245–256.

Emoto K, Parrish JZ, Jan LY, Jan YN. 2006. The tumour suppressor Hippo acts with the NDR kinases in dendritic tiling and maintenance. *Nature* **443:** 210–213.

Fradkin LG, Noordermeer JN, Nusse R. 1995. The *Drosophila* Wnt protein DWnt-3 is a secreted glycoprotein localized on the axon tracts of the embryonic CNS. *Dev Biol* **168:** 202–213.

Fradkin LG, Dura JM, Noordermeer JN. 2010. Ryks: new partners for Wnts on the developing and regenerating nervous system. *Trends Neurosci* **33:** 84–92.

Fuerst PG, Bruce F, Tian M, Wei W, Elstrott J, Feller MB, Erskine L, Singer JH, Burgess RW. 2009. DSCAM and DSCAML1 function in self-avoidance in multiple cell types in the developing mouse retina. *Neuron* **64:** 484–497.

Furrer MP, Vasenkova I, Kamiyama D, Rosado Y, Chiba A. 2007. Slit and Robo control the development of dendrites in *Drosophila* CNS. *Development* **134:** 3795–3804.

Gao FB, Kohwi M, Brenman JE, Jan LY, Jan YN. 2000. Control of dendritic field formation in *Drosophila*: the roles of flamingo and competition between homologous neurons. *Neuron* **28:** 91–101.

Gibson DA, Tymanskyj S, Yuan RC, Leung HC, Lefebvre JL, Sanes JR, Chedotal A, Ma L. 2014. Dendrite self-avoidance requires cell-autonomous Slit-Robo signaling in cerebellar Purkinje cells. *Neuron* **81:** 1040–1056.

Grueber WB, Ye B, Moore A, Jan LY, Jan YN. 2003. Dendrites of distinct classes of *Drosophila* sensory neurons show different capacities for homotypic repulsion. *Curr Biol* **13:** 616–626.

Hadjieconomous D, Rotkopf S, Alexandre C, Bell DM, Dickson BJ, Salecker I. 2011. Flybow: genetic multicolor cell labeling for neural circuit analysis in *Drosophila melanogaster*. *Nat Methods* **8:** 260–266.

Hughes ME, Bortnick R, Tsubouchi A, Baumer P, Kondo M, Uemura T, Schmucker D. 2007. Homophilic Dscam interactions control complex dendrite morphogenesis. *Neuron* **54:** 417–427.

Hutchins BI, Li L, Kalil K. 2011. Wnt/calcium signaling mediates axon growth and guidance in the developing corpus callosum. *Dev Neurobiol* **71:** 269–283.

Jan YN, Jan LY. 2010. Branching out: mechanisms of dendritic arborization. *Nat Rev Neurosci* **11:** 316–328.

Kanamori T, Kanai M, Dairyo Y, Yasunaga K, Morikawa R, Emoto K. 2013. Compartmentalized calcium transients trigger dendrite pruning in *Drosophila* sensory neurons. *Science* **340:** 1475–1478.

Kanamori T, Yoshino J, Yasunaga K, Dairyo Y, Emoto K. 2015. Local endocytosis triggers dendritic thinning and branching in *Drosophila* sensory neurons. *Nat Commun* **6:** 6515.

Kaufmann WE, Moser HW. 2000. Dendritic anomalies in disorders associated with mental retardation. *Cereb Cortex* **10:** 981–991.

Kikuchi A, Yamamoto H, Kishida S. 2007. Multiplicity of the interactions of Wnt proteins and their receptors. *Cell Signal* **19:** 659–671.

Koike-Kumagai M, Yasunaga K, Morikawa R, Kanamori T, Emoto K. 2009. The target of rapamycin complex 2 controls dendritic tiling of *Drosophila* sensory neurons through the Tricornered kinase signaling pathway. *EMBO J* **28:** 3879–3892.

Kopp A, Blackman RK, Duncan I. 1999. Wingless, Decapantaplegic and EGF Receptor signaling pathways interact to specify dorso-ventral pattern in the adult abdomen of *Drosophila*. *Development* **126:** 3495–3507.

Kuo CT, Jan LY, Jan YN. 2005. Dendrite-specific remodeling of *Drosophila* sensory neurons requires matrix metalloproteases, ubiquitin–proteasome, and exdysone signaling. *Proc Natl Acad Sci* **102:** 15230–15235.

Lee T, Luo L. 1999. Mosaic analysis with repressible cell marker for studies of gene function in neuronal morphogenesis. *Neuron* **22:** 451–461.

Lee T, Winter C, Marticke SS, Lee A, Luo L. 2000. Essential roles of *Drosophila* RhoA in the regulation of neuroblast proliferation and dendritic but not axonal morphogenesis. *Neuron* **25:** 307–316.

Lefebvre JL, Kostadinov D, Chen WV, Maniatis T, Sanes JR. 2012. Protocadherins mediate dendritic self-avoidance in the mammalian nervous system. *Nature* **488:** 517–521.

Lin B, Wang SW, Masland RH. 2004. Retinal ganglion cell type, size, and spacing can be specified independent of homotypic dendritic contacts. *Neuron* **43:** 475–485.

Liu Y, Shi J, Lu CC, Wang ZB, Lyuksyutova AI, Song XJ, Zou Y. 2005. Ryk-mediated Wnt repulsion regulates posterior-directed growth of corticospinal tract. *Nat Neurosci* **8:** 1151–1159.

Luo L. 2000. Rho GTPases in neuronal morphogenesis. *Nat Rev Neurosci* **1:** 173–180.

Masland RH. 2012. The neuronal organization of the retina. *Neuron* **76:** 266–280.

Matsubara D, Horiuchi SY, Shimono K, Usui T, Uemura T. 2011. The seven-pass transmembrane cadherin Flamingo controls dendritic self-avoidance via its binding to a LIM domain protein, Espinas, in *Drosophila* sensory neurons. *Genes Dev* **25:** 1982–1996.

Matsuoka RL, Jiang Z, Samuels IS, Ngyuyen-Ba-Charvet KT, Sun LO, Peachey NS, Chedotal A, Yau KW, Kolodkin AL. 2012. Guidance-cue control of horizontal cell morphology, lamination, and synapse formation in the mammalian outer retina. *J Neurosci* **32:** 6859–6868.

Matthews BJ, Kim ME, Flanagan JJ, Hattori D, Clemens JC, Zipursky SL, Grueber WG. 2007. Dendrite self-avoidance is controlled by Dscam. *Cell* **129:** 593–604.

Moreau-Fauvarque C, Talliebourg E, Boissoneau E, Mesnard J, Dura JM. 1998. The receptor tyrosine kinase gene linotte is

required for neuronal pathway selection in the *Drosophila* mushroom bodies. *Mech Dev* **78:** 47–61.

Morikawa R, Kanamori T, Yasunaga K, Emoto K. 2011. Different levels of the TRIM protein Asap regulate distinct axonal projections of *Drosophila* sensory neurons. *Proc Natl Acad Sci* **108:** 19389–19394.

Parrish JZ, Emoto K, Kim MD, Jan YN. 2007. Mechanisms that regulate establishment, maintenance, and remodeling of dendritic fields. *Annu Rev Neurosci* **30:** 399–423.

Perry VH, Linden R. 1982. Evidence for dendritic competition in the developing retina. *Nature* **297:** 683–685.

Polleux F, Morrow T, Ghosh A. 2000. Semaphorin 3A is a chemoattractant for cortical apical dendrites. *Nature* **404:** 567–573.

Puram SV, Bonni A. 2013. Cell-intrinsic driver of dendrite morphogenesis. *Development* **140:** 4657–4671.

Purpura DP. 1975. Dendritic differentiation in human cerebral cortex: normal and aberrant developmental patterns. *Adv Neurol* **12:** 91–134.

Schmidt S, Debant A. 2014. Function and regulation of the Rho guanine nucleotide exchange factor Trio. *Small GTPases* **5:** e29769.

Shimizu K, Sato M, Tabata T. 2011. The Wnt5/planar cell polarity pathway regulates axonal development of the *Drosophila* mushroom body neuron. *J Neurosci* **31:** 4944–4954.

Shimono K, Fujimoto A, Tsuyama T, Yamamoto-Kochi M, Sato M, Hattori Y, Sugimura K, Usui T, Kimura K, Uemura T. 2009. Multidendritic sensory neurons in the adult *Drosophila* abdomen: origin, dendritic morphology, and segment- and age-dependent programmed cell death. *Neural Dev* **4:** 37.

Shirras AD, Couso JP. 1996. Cell fates in the adult abdomen of *Drosophila* are determined by wingless during pupal development. *Dev Biol* **175:** 24–36.

Smith HK, Roberts IL, Allen MJ, Connolly JB, Moffat KG, O'Kane CJ. 1996. Inducible ternary control of transgene expression and cell ablation in *Drosophila*. *Dev Genes Evol* **206:** 14–24.

Smith CJ, Watson JD, VanHoven MK, Colon-Ramos DA, Miller DM III. 2012. Netrin (UNC-6) mediates dendritic self-avoidance. *Nat Neurosci* **15:** 731–737.

Soba P, Zhu S, Emoto K, Younger S, Yang SJ, Yu HH, Lee T, Jan LY, Jan YN. 2007. *Drosophila* sensory neurons require Dscam for dendrite self-avoidance and proper dendritic organization. *Neuron* **54:** 403–416.

Sonoshita M, Itatani Y, Kakizaki F, Sakimura K, Terashima T, Katsuyama Y, Sakai Y, Taketo MM. 2014. Promotion of colorectal cancer invasion and metastasis through activation of Notch–Dab1–Abl–RhoGEF protein TRIO. *Cancer Discov* **5:** 198–211.

Srahna M, Leyssern M, Choi CM, Fradkin LG, Noordermeer JN, Hassan BA. 2006. A signaling network for patterning of neuronal connectivity in the *Drosophila* brain. *PLoS Biol* **4:** e348.

Sun LO, Jang Z, Rivlin-Etzion M, Hand R, Brady CM, Matsuoka RL, Yau KW, Feller MB, Kolodkin AL. 2013. On and off retinal circuit assembly by divergent molecular mechanisms. *Science* **342:** 1241974.

Venken KJ, He Y, Hoskins RA, Bellen HJ. 2006. P[acman]: a BAC transgenic platform for targeted insertion of large DNA fragments in *D. melanogaster*. *Science* **314:** 1747–1751.

Wassle H, Boycott BB. 1991. Functional architecture of the mammalian retina. *Physiol Rev* **71:** 447–480.

Wong RO, Ghosh A. 2002. Activity-dependent regulation of dendritic growth and patterning. *Nat Rev Neurosci* **3:** 803–812.

Wouda RR, Bansraj MR, de Jong AW, Noordermeer JN, Frandkin LG. 2008. Src family kinases are required for WNT5 signaling through the Derailed/RYK receptor in the *Drosophila* embryonic central nervous system. *Development* **135:** 2277–2287.

Wu Y, Helt JC, Wexler E, Petrova IM, Noordermmer JN, Fradkin LG, Hing H. 2014. Wnt5 and drl/ryk gradients pattern the *Drosophila* olfactory map. *J Neurosci* **34:** 14961–14972.

Yasunaga K, Kanamori T, Morikawa R, Suzuki E, Emoto K. 2010. Dendrite reshaping of adult *Drosophila* sensory neurons requires matrix metalloproteinase-mediated modification of the basement membranes. *Dev Cell* **18:** 621–632.

Yoshikawa S, McKinnon RD, Kokei M, Thomas JB. 2003. Wnt-mediated axon guidance via the *Drosophila* Derailed receptor. *Nature* **422:** 583–588.

Zipursky SL, Grueber WB. 2013. The molecular basis of self-avoidance. *Annu Rev Neurosci* **36:** 547–568.